

# Luminescence of Tiopronin Monolayer-Protected Silver Clusters Changes To That of Gold Clusters upon Galvanic Core Metal Exchange<sup>†</sup>

Tao Huang and Royce W. Murray\*

Kenan Laboratories of Chemistry, University of North Carolina, Chapel Hill, North Carolina 27599-3290

Received: December 11, 2002; In Final Form: March 18, 2003

Water-soluble tiopronin monolayer-protected silver clusters (Ag MPCs), with 1.6 nm average diameter cores, exhibit visible luminescence at 500 nm with a quantum yield estimated near  $10^{-4}$  when excited at 400 nm. The Ag MPCs become organic-soluble upon conversion to poly(ethylene glycol) quaternary ammonium salts of the carboxylates of the *N*-2-mercaptopropionylglycine ligand monolayer. The Ag MPC luminescence becomes more intense in nonpolar organic solvents. The luminescence may arise from interband recombination transitions between the d band and the sp conduction band. Atoms in the Ag MPC core can be replaced by Au atoms via a galvanic metal exchange reaction between the silver clusters and Au(I)[SCH<sub>2</sub>(C<sub>6</sub>H<sub>4</sub>)C(CH<sub>3</sub>)<sub>3</sub>]. The reaction was detected by observing the time-dependent change of the surface plasmon absorbance and emission spectra of the Ag MPC to spectra characteristic of Au MPCs. The reaction was also assessed by transmission electron microscopy (TEM) and elemental analysis.

The luminescence of silver metal<sup>1</sup> and generally that of noble metals is generally attributed to electronic transitions between the upper d band and conduction sp band.<sup>2</sup> Luminescence of silver can be induced by irradiating the metal surface or film with electron,<sup>3–7</sup> photon,<sup>8</sup> or laser beams,<sup>2,9–11</sup> with reported emission peak positions distributed over a wide range, 320–520 nm. A considerable interest in luminescence from silver has been related to roughened silver surfaces or supported silver nanoparticles, which enhance efficiencies of absorbance and emission via localized plasmon resonances and are used in surface-enhanced Raman scattering (SERS).<sup>12,13</sup> Silver films are also used in surface plasmon resonance spectroscopy (SPR).<sup>14</sup> Little, however, has been reported about luminescence from silver particles, especially Ag nanoparticles (aside from cases where the luminescence originates from molecular fluorophores supported on silver nanoparticles<sup>15</sup>). Lee<sup>16</sup> observed 460 nm luminescence of aqueous silver colloids and powders using a N<sub>2</sub> laser at 337.1 nm and a XeCl gas excimer laser at 308 nm and related the luminescence to surface plasmon resonance and interband transitions. Recently, several groups have reported fluorescence of very small silver clusters (Ag<sub>2</sub> to Ag<sub>30</sub>) formed in rare gas droplets.<sup>17</sup>

More is known about luminescence from gold nanoparticles. While Mooradian<sup>2</sup> interpreted the luminescence of noble metal surfaces as an excitation of electrons from occupied d bands into sp states above the Fermi level (interband transitions), it is now known to be overlaid with numerous chemical effects, especially for luminescence from gold nanoparticles. Wilcoxon et al.<sup>18</sup> reported emission at 440 nm (excited at 230 nm) from citrate-stabilized gold nanoparticles (diameter < 5 nm) but occurring above 600 nm when dodecanethiol was introduced into the high-performance liquid chromatographic (HPLC) mobile phase. Coupling to the field of excited surface plasmon resonances can, in the case of gold nanorods, strongly enhance the luminescence efficiency.<sup>19</sup> Bigioni et al.<sup>20</sup> recently reported lower energy (ca. 1.1 eV, near-infrared, excited at 1.06  $\mu$ m)

luminescence from dodecanethiolate-protected small gold nanocrystals and suggested the role of sp intraband transitions in the emission. Our laboratory<sup>21</sup> observed visible (770 nm, 1.6 eV) luminescence of tiopronin monolayer-protected gold clusters (Au MPCs, 1.8 nm avg. core diameter). While attributing it to a d–sp interband transition, we pointed<sup>21</sup> to the further complexity suggested by the strong variation of the luminescence maximum among MPCs stabilized by different but structurally related thiolate ligands. Link et al.<sup>22</sup> observed two emission transitions for a glutathione-protected 0.9 nm core size Au MPC: that at 1.55 eV was discussed as a sp  $\rightarrow$  d band radiative recombination and the lower energy emission at 1.15 eV as an intra-sp band transition across a highest occupied–lowest unoccupied molecular orbital (HOMO–LUMO) gap. Since this nanoparticle contained only 28 Au core atoms, an alternative, molecular analysis was also discussed.

Monolayer-protected metal clusters (MPCs) offer a wide range of chemistry via manipulation of the monolayer (often thiolate ligands) composition.<sup>23</sup> MPCs have been discussed<sup>21–25</sup> in the contexts, among others, of nanoscale electronic devices, multifunctional catalysts, and chemical sensors. In these contexts, new nanoparticle materials that exhibit easily detected optical responses are of substantial interest. The sole previous instance of metal-based emission observed from Ag MPCs (dodecanethiolate-coated, 4 nm diameter) was in scanning tunneling microscopy- (STM-) induced photoemission experiments by Taleb et al.,<sup>26</sup> where only total emission was recorded.

Reported here are the synthesis and spectroscopy of three somewhat polydisperse, air-stable, water-soluble tiopronin (*N*-2-mercaptopropionylglycine) monolayer-protected silver clusters (Ag MPC), in which the *average* Ag core sizes are  $1.6 \pm 0.7$ ,  $3.0 \pm 0.9$ , and  $4.8 \pm 1.0$  nm. The surface plasmon absorbance excitation and the fluorescence excitation maxima shift with average nanoparticle size, but shift of the emission maxima with average size was not detected. The luminescence quantum yields (ca.  $10^{-4}$ ) increase slightly with decreasing core size and the emission becomes more intense in less polar organic solvents. Also demonstrated is replacement of about two-thirds of the

<sup>†</sup> Part of the special issue "Arnim Henglein Festschrift".

\* Corresponding author: e-mail rwm@email.unc.edu.

core Ag atoms by Au atoms, via a galvanic reaction<sup>27</sup> between the Ag MPC core and a Au<sup>I</sup> thiolate salt, Au(I)[SCH<sub>2</sub>(C<sub>6</sub>H<sub>4</sub>)C(CH<sub>3</sub>)<sub>3</sub>]. The reaction mixture contains a 1:1 mole ratio of Au(I) complexes and core Ag atoms. The formation of the resulting bimetal Ag/Au MPC was tracked by observing the characteristic UV-vis and luminescence spectra of the Ag MPC change into those of Au tiopronin-coated MPC. The bimetal product was also analyzed by transmission electron microscopy (TEM) and elemental analysis. The absence of characteristic Ag MPC absorption or emission spectra after one-day galvanic exchange reaction suggests roughly complete replacement of Ag atoms originally on the MPC core surface.

## Experimental Section

**Chemicals.** Silver nitrate (AgNO<sub>3</sub>, 99.9999%) and *N*-(2-mercaptopropionyl)glycine (tiopronin, 99%) were purchased from Aldrich. House-distilled water was purified on a Barnstead NANOpure system ( $\geq 18$  M $\Omega$ ). All other chemicals were reagent grade and used as received.

**Synthesis of Tiopronin Monolayer-Protected Silver Clusters.** The Ag MPC synthesis parallels that of the related tiopronin-coated Au MPCs.<sup>21,29</sup> In a typical reaction, solutions of 1 g of AgNO<sub>3</sub> dissolved in 50 mL of H<sub>2</sub>O (5.89 mmol), 2.88 g of tiopronin dissolved in 20 mL of H<sub>2</sub>O (17.6 mmol, mole ratio thiol/Ag = 3), and 0.6 g of NaBH<sub>4</sub> dissolved in 15 mL of H<sub>2</sub>O (15.9 mmol), all cooled to under 0 °C, were mixed. This reaction is termed a 3 $\times$  preparation; reactions were also run at thiol/Ag mole ratios of 1:1 (1 $\times$ ) and 2:1 (2 $\times$ ) and the same mole ratio of reductant to Ag. The tiopronin solution was added to the silver solution, followed immediately afterward by the NaBH<sub>4</sub> solution. The resulting black solution was stirred vigorously for an additional 30 min at 0 °C. The Ag MPCs were precipitated by adding 300 mL of methanol, then filtered and washed sequentially with methanol, ethanol, and acetone. The black silver MPC powders were then redissolved in H<sub>2</sub>O and dialyzed (8 in. Spectra/Por CE, MWCO = 5000) over a 3-day period. The water was removed under vacuum below 30 °C. Dialysis does not cause MPC decomposition/aggregation since dissociation of the tiopronin ligands from the Ag cores appears to be minor. The product material was spectroscopically pure by NMR (absence of sharp resonance peaks of unreacted thiol or disulfide byproducts). Luminescence can be observed both immediately after MPC formation and after the preceding purification, and as was the case for Au tiopronin MPCs,<sup>21</sup> luminescence is absent if any of the reaction ingredients are omitted.

**Synthesis of Triethylammonium MePEG-350 Hydroxide.** MePEG-350 was converted to (MePEG-Et<sub>3</sub>N<sup>+</sup>)(tosylate<sup>-</sup>) according to a published procedure.<sup>30</sup> The tosylate anion was replaced with hydroxide anion by use of Dowex 1  $\times$  8–400 ion-exchange resin (Aldrich) prepared according to standard procedures. The (MePEG-Et<sub>3</sub>N<sup>+</sup>)(OH<sup>-</sup>) was used as a dilute solution obtained directly from the ion-exchange column.

**Synthesis of Au(I)[*p*-SCH<sub>2</sub>(C<sub>6</sub>H<sub>4</sub>)C(CH<sub>3</sub>)<sub>3</sub>].** Tetrachloroauric acid (0.31 g) and *p*-HSCH<sub>2</sub>(C<sub>6</sub>H<sub>4</sub>)C(CH<sub>3</sub>)<sub>3</sub><sup>28</sup> (0.43 g) were added to 30 mL of ethanol at 50 °C, forming a white precipitate, which was collected after 10 min, and the precipitate was washed with 200 mL each of ethanol, acetone, and acetonitrile.

**Transmission Electron Microscopy.** TEM samples were prepared by placing a single drop of a ca. 1 mg/mL aqueous MPC solution onto Formvar-coated (200–300 Å) copper grids (200 mesh), waiting 5 min, and removing excess solution by touching a small piece of filter paper to the edge of the grid. The grid was further dried under N<sub>2</sub> flow or in air for 30 min.

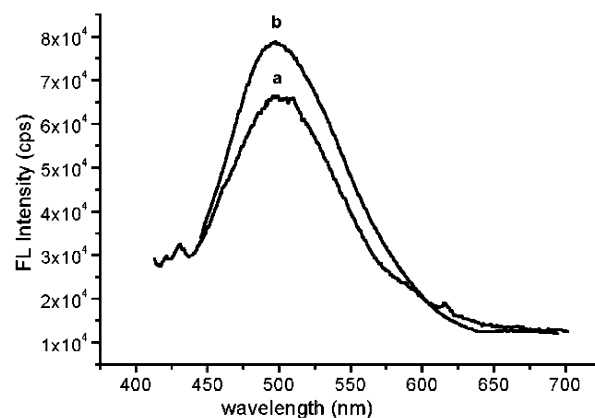


**Figure 1.** Luminescence spectra of 1.6 nm average core size tiopronin-coated Ag MPCs: (a) aqueous, 1.0  $\mu$ M; (b) in CH<sub>2</sub>Cl<sub>2</sub>, 1.0  $\mu$ M.

Phase-contrast images of the MPCs were obtained with a side-entry Phillips CM12 electron microscope operating at 120 keV. Three typical regions of each sample were imaged at either 300K or 560K magnification. Histograms of Ag core sizes were based on at least two digitized photographic enlargements, analyzed with Scion Image Beta Release 2 (available at [www.scioncorp.com](http://www.scioncorp.com)). Small populations of MPCs larger than about 5 nm core diameter are thought to be due to adventitious core aggregation and are excluded from the core diameter averages in Figure 3c,d. The 3 $\times$ , 2 $\times$ , and 1 $\times$  syntheses produced MPCs with average TEM core diameters of  $1.6 \pm 0.7$ ,  $3.0 \pm 0.9$ , and  $4.8 \pm 1.0$  nm.

**Spectroscopic Measurements.** Proton NMR spectra were recorded at 200 MHz on a Bruker AC200 NMR spectrometer at room temperature in concentrated D<sub>2</sub>O solutions. A line broadening factor of 1 Hz was used to improve NMR signal-to-noise (S/N) and a relaxation delay of 5 s was used to allow adequate signal decay between pulses. UV-vis spectra (200–800 nm) were collected with an ATI Unicam UV4 spectrometer. Luminescence spectra were taken at a standard right angle (RA) configuration on an ISA Instruments Jobin Yvon-Spex Fluorolog model FL3-21 spectrometer.

## Results and Discussion

**Spectra of Water-Soluble Ag MPC Solutions.** During the synthesis of the Ag MPCs, small volumes ( $\sim 1.5$  mL) of all the reagent solutions involved were tested for fluorescence. There was no emission until sodium borohydride was added to the silver-thiol mixture. Figure 1 shows the luminescence spectrum from a yellow-colored 1  $\mu$ M (cluster concentration, if not specified otherwise) tiopronin-coated Ag MPC solution (3 $\times$  preparation, excited at 380 nm). The broad emission peak is centered at ca. 500 nm (2.5 eV). The intensity is accurately proportional to the Ag MPC concentration as shown in Figure 2, at least for low concentrations. At higher concentrations the emission intensity plot tends to fold over, reaching a maximum at about 10  $\mu$ M in MPCs. Like tiopronin-coated Au MPCs,<sup>21</sup> the Ag MPCs are strong absorbers; a 1 mM MPC solution is opaque black. Following a previous analysis,<sup>31</sup> the nonlinearity at higher concentrations for Ag MPCs is attributed to some combination of self-absorbance and self-quenching of tiopronin-MPCs.

Monolayer-protected metal clusters are thought<sup>23</sup> to assemble by a core nucleation-growth-passivation sequence; higher mole ratios of thiol to metal salt should accordingly produce MPCs with smaller metal cores. This has been observed<sup>32</sup> for Au MPCs, and we find it also for the tiopronin-coated Ag MPCs;

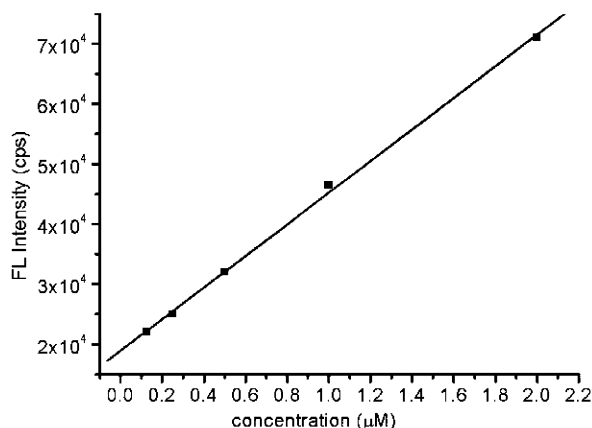


**Figure 2.** Luminescence intensity vs concentration of tiopronin-coated Ag MPCs (1.6 nm average core diameter). *R* of linear fit was 0.99932.

**TABLE 1: Spectral Properties of Tiopronin-Coated Ag MPCs**

preparation <sup>a</sup>	size <sup>b</sup> (nm)	plasmon absorbance $\lambda_{\text{max}}^c$ (nm)	excitation $\lambda_{\text{max}}^d$ (nm)	emission $\lambda_{\text{max}}$ (nm)	quantum yield <sup>e</sup>
3×	1.6 ± 0.7	380	372	500	9.0 × 10 <sup>-5</sup>
2×	3.0 ± 0.9	390	386	500	8.2 × 10 <sup>-5</sup>
1×	4.8 ± 1.0	396	400	500	8.0 × 10 <sup>-5</sup>

<sup>a</sup> Ratio of thiol to AuCl<sub>4</sub><sup>-</sup> in the synthesis; see Experimental Section.

<sup>b</sup> From TEM, see Figure 3A–C. <sup>c</sup> From Figure 4A. <sup>d</sup> From Figure 4B.

<sup>e</sup> At 500 nm, with excitation at 380 nm.

3×, 2×, and 1× preparations generate Ag MPCs with average core diameters of 1.6 ± 0.7, 3.0 ± 0.9, and 4.8 ± 1.0 nm, respectively. These average dimensions were established by transmission electron microscopy (TEM) images as in Figure 3a–c. The images show that the Ag MPCs are moderately polydisperse, and many of the cores are spaced apart from one another by roughly uniform distances. The spacing is caused<sup>32</sup> by the surrounding tiopronin monolayers, which are not visualized in these TEM images.

Absorbance spectra of the different core size Ag MPCs are shown in Figure 4A. The peak near 400 nm (3.1 eV) is the surface plasmon absorbance, a collective excitation of conduction electrons. Judging from the low-energy absorbance tail in the spectrum, the separation of d → sp band edges lies at much lower energy, below 600–700 nm. The surface plasmon band shifts to slightly lower energy with increasing core size; the peaks lie at 380, 390, and 396 nm for the 1.6, 3.0, and 4.8 nm average diameter tiopronin-coated Ag MPCs (Table 1). This shift in plasmon excitation energy, ca. −0.04 eV/nm of MPC core diameter, suggests that the consequence of the Ag–S bond's electron donation to the nanoparticle—which is proposed<sup>33,34</sup> to effect a blue shift—is enhanced for smaller nanoparticles. The only other study of plasmon band position for thiolate-coated Ag MPCs of size comparable to those discussed here observed<sup>18</sup> a shift in the opposite direction (ca. 0.06 eV/nm of MPC core diameter) for Ag MPCs separated by size-exclusion chromatography. The monolayer in that study was the relatively nonpolar dodecanethiolate. Haynes and Van Duyne<sup>33b</sup> have documented the complex sensitivity of supported Ag nanoparticles to their nanoenvironment.

Excitation spectra (Figure 4B) for the Ag MPC fluorescence (detected at 500 nm) exhibit maxima that are very close to the energies of the surface plasmon absorbance peaks (Table 1) and are similarly red-shifted with increase in Ag MPC core size. The excitation bands appear to be broad, but curves b and (more

clearly) c consist of multiple peaks. The higher energy (shoulder) peak in curve c, for the larger average core size Ag MPC, is at the same energy as the excitation peak for the smallest core size (curve a). We believe this simply reflects the polydispersity of the Ag MPC sample, in which the higher energy shoulder in curve c corresponds to the smaller core size subpopulation of that sample (see Figure 3A).

The quantum yield of the 0.5 μM tiopronin-coated Ag MPC solution emissions were estimated by comparing their intensities with that at 630 nm of standard 1 μM solutions of tris(2,2'-bipyridine)ruthenium(II) dichloride (excited at 450 nm, an absorption maximum of this compound.) The quantum yield of the Ru complex emission is 0.042<sup>35</sup> under these conditions. These emission spectra fall into a very flat response wavelength range of the spectrofluorometer's PMT. The Ag MPC quantum yields for emission at 500 nm and excitation at 380 nm, reported in Table 1, increase slightly with decreasing core size, but the emission energy seems not to vary with average core size. The quantum yields are ca. 10-fold lower than that for the analogous tiopronin-coated Au MPC.<sup>21</sup> The polydispersity of the MPCs must of course be kept in mind when considering these results.

The emission from the tiopronin-coated Ag MPCs is plausibly attributed to an interband recombination of holes in the d band with electrons in sp levels, as with tiopronin gold MPCs. The closeness of the plasmon absorbance and excitation peak energies, however, strongly suggests that the interband transition intensity is promoted by coupling with the surface plasmon resonance excitation. This explanation parallels the detailed analysis given<sup>19</sup> to the strong emission from gold nanorods, except that there is no aspect ratio-related enhancement in the present case.

**Solvent and pH Dependence of Ag MPC Emission.** Figure 5 shows how the fluorescence intensity of 1.1 μM (aq) Ag MPCs with 1.6 nm average core diameter changes with pH. The drop in fluorescence intensity at high pH is not fully reversible (returns to 87% of its original value at pH 7) so some decomposition process may be at work. At pH < 5, the tiopronin-coated Ag MPCs tend to precipitate from aqueous solution but readily redissolve (with 23% fluorescence recovery to its original value at pH 7) if the pH is made more basic. It seems that some small degree of carboxylic acid dissociation aids the Ag MPC solubility.

The tiopronin-coated Ag MPCs are not soluble in organic solvents, but like DNA,<sup>36</sup> the conjugate base can be converted to an organic-soluble form by providing an appropriate cation. Thus, when a stoichiometric amount of triethyl(MePEG350)-ammonium hydroxide (see Experimental Section) was added to an aqueous solution of 1.6 nm core diameter Ag MPCs and the water was removed under vacuum below 30 °C, a black oily solid was obtained that readily dissolves in organic solvents. The maxima for excitation and emission of these Ag MPCs occur at the same energy in organic solvents as in the water-soluble form, but as seen in Figure 1 for CH<sub>2</sub>Cl<sub>2</sub> versus water, and in Table 2 as relative intensities, the emission intensity increases in nonpolar solvents by over 2-fold relative to water. That different solvents can influence the emission probability of tiopronin silver MPCs implies that solvent dipoles can interact to some extent with the surface plasmon resonance field beyond the protecting monolayer.<sup>33b</sup> The extent of the intensity enhancement is (roughly) in order of both static and optical (refractive index squared) constants and seems most consistently ordered for the nonpolar cases. Presumably the interaction through the protecting monolayer occurs through a dispersion force mechanism.

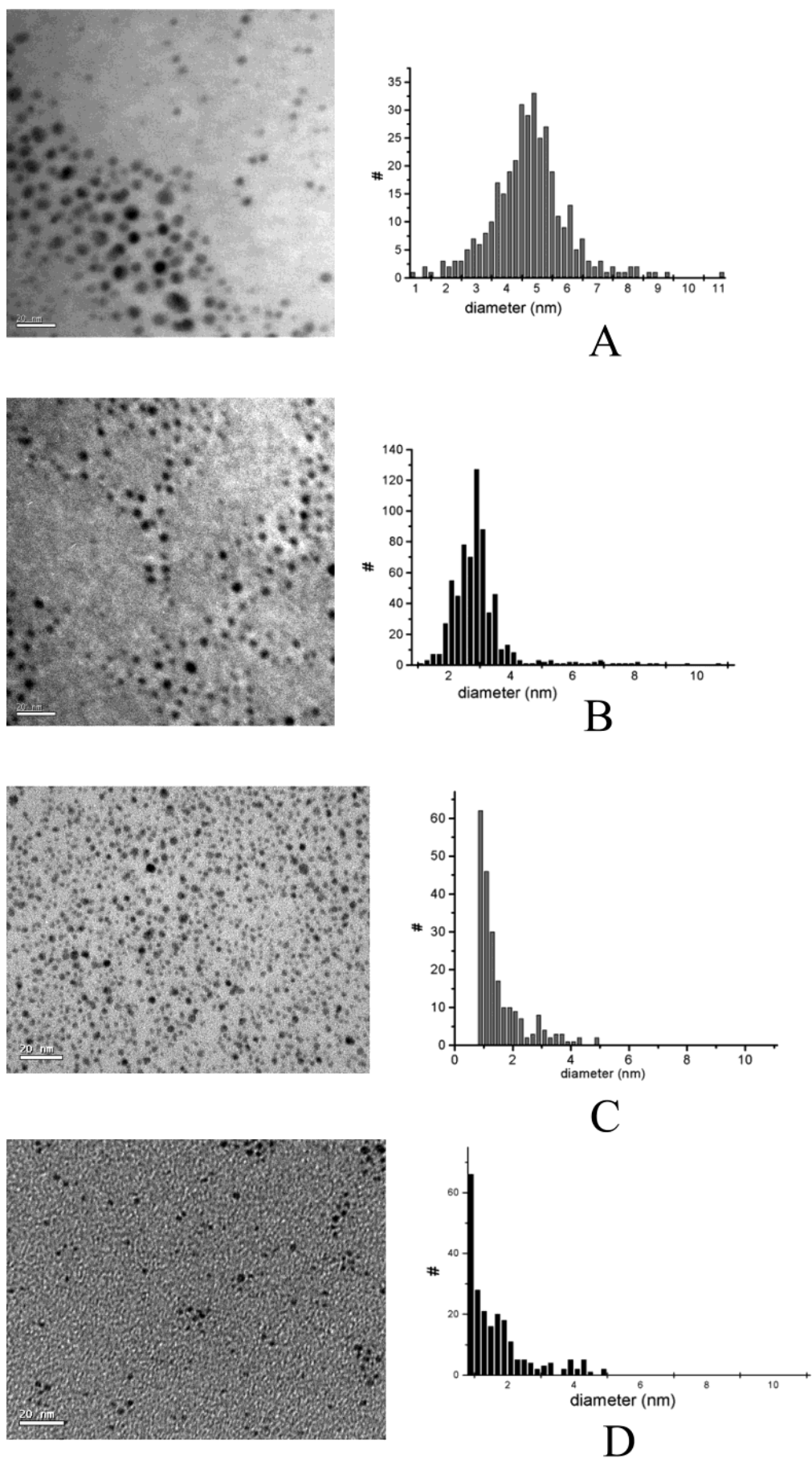


**Figure 3.** Transmission electron micrographs and size histograms of tiopronin-coated Ag MPCs. (A) 1 $\times$  preparation, avg. diameter =  $4.8 \pm 1.0$  nm; (B) 2 $\times$  preparation,  $3.0 \pm 0.9$  nm; (C) 3 $\times$  preparation,  $1.6 \pm 0.7$  nm; (D) 3 $\times$  preparation after 1 day of galvanic exchange reaction,  $1.6 \pm 0.9$  nm.



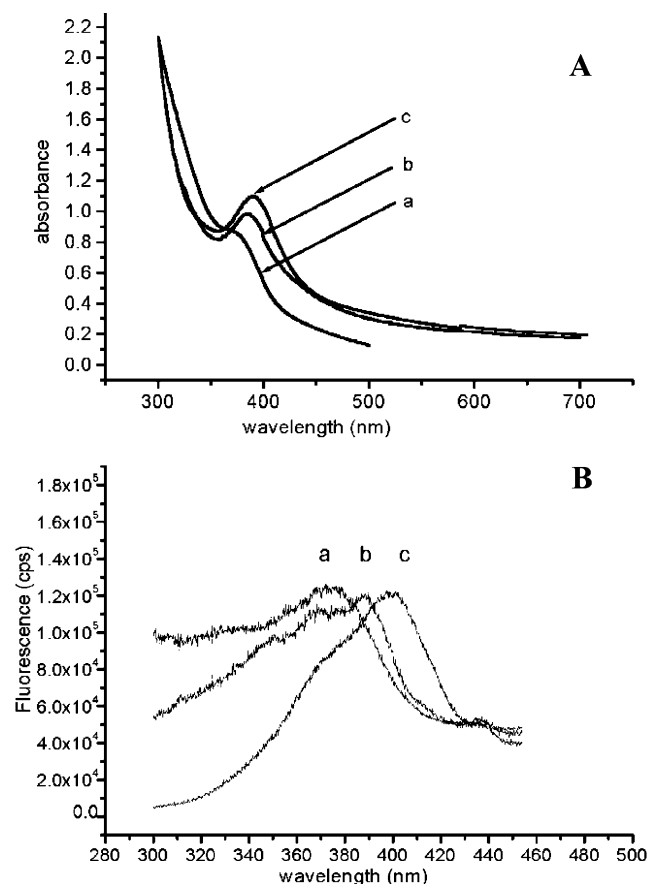


**Figure 4.** (A) UV-Vis absorbance spectra and (B) excitation spectra of emission detected at 500 nm of tiopronin-coated Ag MPCs, with (a) 1.6 nm, (b) 3.0 nm, and (c) 4.8 nm average core diameters.

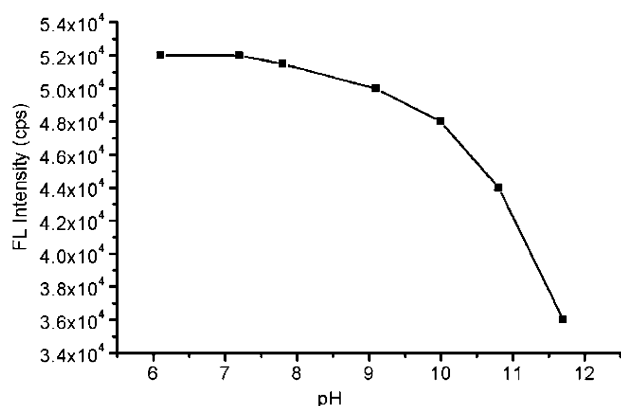


**Figure 5.** Luminescence intensity of  $\approx 1.1 \mu\text{M}$  tiopronin-coated Ag MPC solution (1.6 nm average core diameter) versus pH.

**Core Metal Galvanic Exchange Reaction.** It is expected that metal MPCs would react with salts of more noble metals. This was demonstrated recently<sup>27</sup> in toluene- and  $\text{CH}_2\text{Cl}_2$ -phase reactions of dodecanethiolate monolayer-protected Ag, Pd, and Cu MPCs with the thiolate complex  $\text{Au}(\text{I})[\text{SCH}_2\text{C}_6\text{H}_4\text{C}(\text{CH}_3)_3]$ . The organic-soluble tiopronin-coated Ag MPCs also react with  $\text{Au}(\text{I})[\text{SCH}_2(\text{C}_6\text{H}_4)\text{C}(\text{CH}_3)_3]$  to form bimetal core Ag/Au MPCs, as cartooned in Scheme 1 (tiopronin ligands not shown).

The reactions were carried out by mixing equal volumes of 8  $\mu\text{M}$  Ag MPC (1.6 nm average diameter) and 1.12 mM  $\text{Au}^{\text{I}}$  compound solutions in  $\text{CH}_2\text{Cl}_2$ . Considering that the average core is  $\text{Ag}_{140}$ , this amounts to a 1:1 mole ratio of  $\text{Au}^{\text{I}}$  and silver<sup>0</sup>, so a stoichiometrically complete galvanic reaction would result in complete replacement of all of the Ag atoms in the Ag MPC

**TABLE 2: Solvent Dependence of Fluorescence at 500 nm of 1.6 nm (avg.) Triethyl(MePEG350)Ammonium Salt of Tiopronin-Coated Ag MPCs**

solvent	rel fluorescence intensity at 500 nm <sup>a</sup>	solvent dielectric constant, $\epsilon_s$	refractive index
water	1.0	78	1.333
ethanol	0.54	24	1.359
acetone	1.0	21	1.359
$\text{CH}_2\text{Cl}_2$	1.2	9	1.334
THF	2.8	7.5	1.408
toluene	3.6	2.4	1.496

<sup>a</sup> Excited at 380 nm.

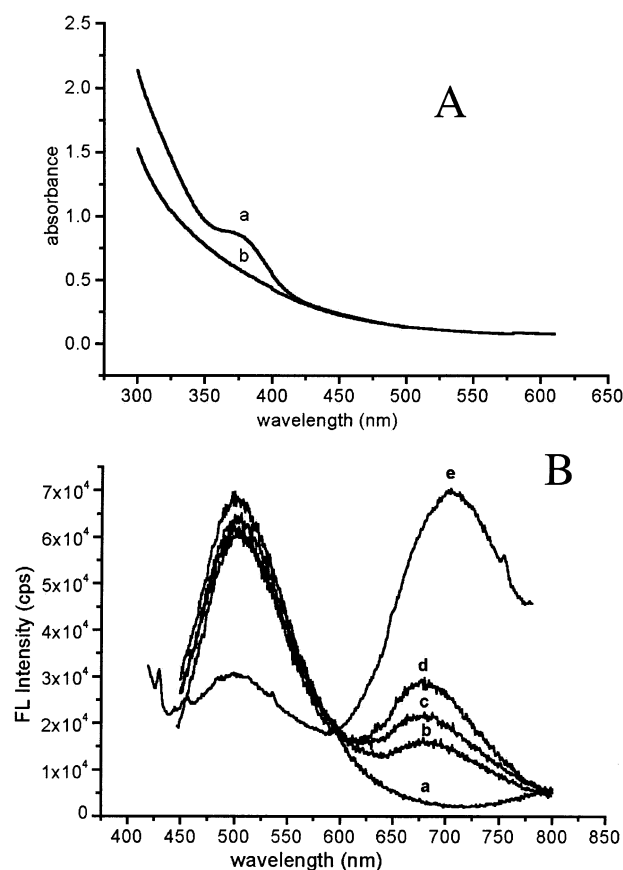
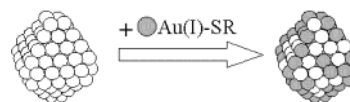


**Figure 6.** (A) Absorbance spectrum of tiopronin-coated Ag MPCs (1.6 nm average core diameter) (a) before galvanic exchange and (b) after 1 day of reaction. (B) Luminescence of tiopronin-coated Ag MPCs (1.6 nm average core diameter) (a) before galvanic exchange, (b) after 5 min of reaction, (c) after 10 min of reaction, (d) after 1 h of reaction, and (e) after 1 day of reaction.

#### SCHEME 1



with Au atoms. Figure 6A shows the absorbance spectra of tiopronin-coated Ag MPCs before (curve a) and after (curve b) 1 day of reaction. The surface plasmon band at 380 nm of the tiopronin-coated Ag MPCs decreased with reaction time and after 1 day it had completely disappeared. It is not expected to see a plasmon excitation appear when Au replaces the Ag atoms because Au MPCs of dimensions  $< 2$  nm are too small to display a plasmon peak.<sup>23,29,32</sup> During the galvanic reaction, the emission spectrum (Figure 6B) shows a concurrent decrease at the 500 nm Ag MPC emission energy and the growth of a lower energy

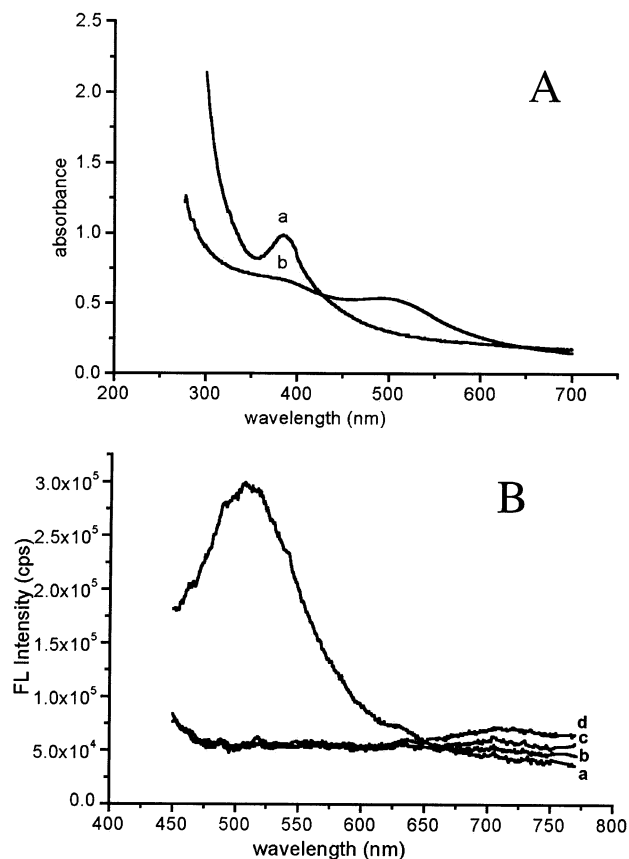


**Figure 7.** (A) Absorbance spectrum of tiopronin-coated Ag MPCs (3.0 nm average core diameter) (a) before galvanic exchange and (b) after 1 day of reaction. (B) Luminescence of tiopronin-coated Ag MPCs (3.0 nm average core diameter) (a) before galvanic exchange, (b) after 1 h of reaction, (c) after 3 h of reaction, and (d) after 1 day of reaction.

emission band at about 670 nm. The 500 nm peak was still present after 1 day of reaction but had been substantially diminished; it disappeared after 2 days of reaction. The lower energy emission peak continued to grow for many hours and after 1 day (curve e) had shifted to ca. 700 nm, whereafter there was no further change (in intensity or energy) over 2 days. Tiopronin-coated Au MPCs emit near 700 nm,<sup>21</sup> so the 700 nm peak can plausibly be interpreted as introduction of gold onto the Ag MPC. Figure 3D shows that the galvanic exchange reaction product consists of nanoparticles with an average diameter of  $1.6 \pm 0.9$  nm, which is indistinguishable from the average diameter of the original tiopronin-coated Ag MPC.

Figure 7 shows an analogous set of galvanic metal exchange results but starting with a larger (3.0 nm average) Ag MPC. In this case, the 390 nm Ag MPC surface plasmon peak decreased over a day of exchange but could still be faintly seen (Figure 7A) after 1 day of reaction. An absorbance peak concurrently appears at ca. 520 nm, which is the usual wavelength for the surface plasmon excitation for tiopronin-coated larger core size Au MPCs ( $>2$  nm diameter).<sup>29</sup> Figure 7B shows that the 500 nm emission peak for the tiopronin-coated 3.0 nm Ag MPC disappears rather quickly after adding the Au<sup>I</sup> thiolate, and after 1 day only a very weak emission peak at about 700 nm can be observed. Larger core size tiopronin-coated Au MPCs do not luminesce<sup>21</sup> in the visible region. The weak emission at 700 nm is likely due to the smaller Ag MPCs in the polydisperse sample that have been exchanged by Au.

The metal content of the galvanic exchange reaction product from the 1.6 nm MPCs (TEM of Figure 3D) was determined by elemental analysis to be a gold to silver atom ratio of 1.55.

On the basis of an average 1.6 nm core size and a corresponding 140 core atom count, and given that the core size did not significantly change after reaction (Figure 3D), this ratio corresponds to a bimetal MPC with an overall composition of about 85 Au and 55 Ag.

Finally, we point to the several interesting questions raised by the loss of the Ag MPC surface plasmon absorbance and emission and the growth in Au MPC emission seen in Figure 6. How many Ag atoms are needed to sustain the plasmon resonance as the Ag MPC is being depleted of its surface atoms? To what extent, if any, do subsurface atoms contribute? What is the sensitivity of the emission process to the Ag and Au atom populations? The emission seems to be dominated by the population of surface atoms, not by the entire core atom population. Further ongoing studies are aimed at these questions, based on more detailed analyses of the time course of core composition and of the spectral changes observed.

**Acknowledgment.** This work was supported in part by grants from the National Science Foundation and Office of Naval Research. We thank the UNC Dental Research Center for access to HRTEM measurements and Brian Nablo for helping with the XPS measurements.

## References and Notes

- Boyd, G. T.; Yu, Z. H.; Shen, Y. R. *Phys. Rev. B* **1986**, *33*, 7923–7936.
- Mooradian, A. *Phys. Rev. Lett.* **1969**, *22*, 185.
- Borziak, B.; Konovalov, I.; Kulypin, Y.; Philipchak, K. *Thin Solid Films* **1976**, *35*, 19.
- Papanicolau, B. G.; Chen, J. M.; Papageorgopoulos, C. A. *J. Phys. Chem. Solids* **1976**, *37*, 403.
- Bonot, A.; Debever, J. M.; Hanus, J. *Solid State Commun.* **1972**, *10*, 173.
- Chung, M. S.; Callcott, T. A.; Kretschmann, E.; Arakawa, E. T. *Surf. Sci.* **1980**, *91*, 245.
- Eesley, G. L. *Phys. Rev. B* **1981**, *24*, 5477.
- Zivitz, M.; Thomas, E. W. *Phys. Rev. B* **1976**, *13*, 2747.
- Wood, T. H.; Klein, M. V. *Solid State Commun.* **1980**, *35*, 263.
- Girlando, A.; Knoll, W.; Philpott, M. R. *Solid State Commun.* **1981**, *38*, 895.
- Von Raben, K. U.; Chang, R. K.; Laube, B. L. *Chem. Phys. Lett.* **1981**, *79*, 465.
- For a comprehensive review see Moskovits, M. *Rev. Mod. Phys.* **1985**, *57*, 783.
- Dick, L. A.; McFarland, A. D.; Van Duyne, R. P. *J. Phys. Chem. B* **2002**, *106* (4), 853–860.
- Davies, J. Surface Plasmon Resonance—The Technique And Its Applications To Biomaterial Processes, *Nanobiology* **1994**, *3* (1), 5–16.
- Stellacci, F.; Bauer, C. A.; Meyer-Friedrichsen, T.; Wenseleers, W.; Marder, S. R.; Perry, J. W. *J. Am. Chem. Soc.* **2003**, *125*, 328–329.
- Lee, K. C. *Surf. Sci.* **1985**, *163* (2–3), L759–L765.
- Ievlev, D.; Rabin, I.; Schulze, W.; Ertl, G. *Eur. Phys. J. D* **2001**, *16*, 157–160.
- Wilcoxon, J. P.; Martin, J. E.; Parsapour, F.; Wiedenman, B.; Kelley, D. F. *J. Chem. Phys.* **1998**, *108*, 9137–9143.
- Mohamed, M. B.; Volkov, V.; Link, S.; El-Sayed, M. A. *Chem. Phys. Lett.* **2000**, *317*, 517–523.
- Bigioni, T. P.; Whetten, R. L.; Dag, O. *J. Phys. Chem. B* **2000**, *104*, 6983–6986.
- Huang, T.; Murray, R. W. *J. Phys. Chem. B* **2001**, *105*, 12498–12502.
- Link, S.; Beeby, A.; Fitzgerald, S.; El-Sayed, M. A.; Schaaff, T. G.; Whetten, R. L. *J. Phys. Chem. B* **2002**, *106*, 3410–3415.
- Templeton, A. C.; Wuelfing, W. P.; Murray, R. W. *Acc. Chem. Res.* **2000**, *33*, 27–36.
- Lyon, L. A.; Musick, M. D.; Natan, M. J. *Anal. Chem.* **1998**, *70*, 5177.
- Lacowicz, J. R.; Shen, Y.; D'Auria, S.; Malicka, J.; Fang, J.; Gryczynski, Z.; Gryczynski, I. *Anal. Biochem.* **2002**, *301* (2), 261–277.
- Taleb, A.; Gusev, A. O.; Silly, F.; Charra, F.; Pileni, M. P. *Appl. Surf. Sci.* **2000**, *162–163*, 553–558.
- Shon, Y.-S.; Dawson, B.; Porter, M.; Murray, R. W. *Langmuir* **2002**, *18*, 3880–3885.
- Al-Sa'dy, A. K. H.; Moss, K.; McAuliffe, C. A.; Parish, R. V. *J. Chem. Soc., Dalton Trans.* **1984**, 1609.

- (29) Templeton, A. C.; Chen, S.; Gross, S. M.; Murray, R. W. *Langmuir* **1999**, *15*, 66–76.
- (30) Dickinson, E. V.; Williams, M. E.; Hendrickson, S. M.; Masui, H.; Murray, R. W. *J. Am. Chem. Soc.* **1999**, *121*, 613–616.
- (31) Aguila, A.; Murray, R. W. *Langmuir* **2000**, *16*, 5949.
- (32) Hostetler, M. J.; Wingate, J. E.; Zhong, C.; Harris, J. E.; Vachet, R. W.; Clark, M. R.; Londono, J. D.; Green, S. J.; Stokes, J. J.; Wignall, G. D.; Glish, G. L.; Porter, M. D.; Evans, N. D.; Murray, R. W. *Langmuir* **1998**, *14*, 17–30.
- (33) (a) Malinsky, M. D.; Kelly, K. L.; Schatz, G. C.; Van Duyne, R. P. *J. Am. Chem. Soc.* **2001**, *123*, 1471–1482. (b) Haynes, C. L.; Van Duyne, R. P. *J. Phys. Chem. B* **2001**, *105*, 5599–5611.
- (34) Linnert, T.; Mulvaney, P.; Henglein, A. *J. Phys. Chem.* **1993**, *97*, 679–682.
- (35) Wilcoxon, J. P.; Martin, J. E.; Parsapour, F.; Wiedenman, B.; Kelley, D. F. *J. Chem. Phys.* **1998**, *108*, 9137.
- (36) Leone, A. M.; Weatherly, S. C.; Williams, M. E.; Thorp, H. H.; Murray, R. W. *J. Am. Chem. Soc.* **2001**, *123*, 218–222.